**ADVANCED
OPTICAL
MATERIALS**

Supporting Information

The Structural Colors of Photonic Glasses

Lukas Schertel, Lukas Siedentop, Janne-Mieke Meijer, Peter Keim, Christof M. Aegerter, Geoffroy J. Aubry, and Georg Maret*

Supporting Information

Scattering Model

Figure SI.1 shows the scattering strength $\lambda/\ell^\star$ calculated by the scattering model introduced in detail in references[1,2] for a particle refractive index $n = 1.6$ and a filling fraction of $f = 0.3$ (black line) plotted versus the size ratio r/λ, with λ the incident wavelength and r the particle radius. The factors $S(\theta)$, $F(\theta)$ or n_{eff} used in the angular integral to calculate $\lambda/\ell^\star$ are respectively set to unity, while keeping the values for the two others (blue, green and grey dashed lines respectively) to show their relevance in the model. We observe that short-range structural correlations accounted for by $S(\theta)$ mainly influence the height and position of the first resonance (green vs. black curve), while Mie scattering in an effective medium represented by the form factor $F(\theta)$ is related to all resonances (blue vs. black). n_{eff} influences both, the height as well as the position of each resonance (dashed grey vs. black). Here the energy coherent potential approximation (ECPA) is used for the calculation of the effective refractive index[1,3] Changing this to the often used Garnett effective index n_{MG} smears out strongly resonant behavior (dotted dashed grey curve).
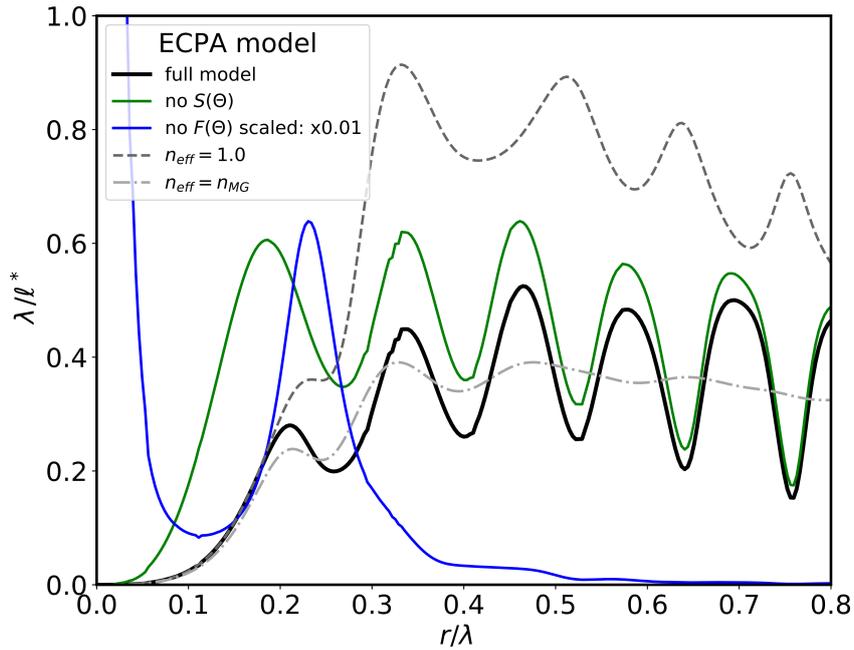
Figure SI.1: Scattering strength $\lambda/\ell^\star$ plotted versus size ratio r/λ for the ECPA scattering model[1,2] for $n = 1.6$ and $f = 0.3$ (black line). The same calculation performed with no structural correlation ($S(\theta) = 1$, green line), no single sphere resonance ($F(\theta) = 1$, blue line, scaled by 0.01) and without an effective index influence ($n_{\text{eff}} = 1$, grey dashed line) as well as using the Maxwell-Garnett value for the effective index ($n_{\text{eff}} = n_{\text{MG}}$, grey dashed dotted line).

Particle Characterization

All PS particles were characterized with TEM to verify their exact size, as the exact particle size is one of the most important parameters determining the structural color of PGs. The size was determined from the TEM micrographs via automated particle detection algorithms in ImageJ to provide the most accurate measurements. Figure SI.2, a) shows a typical TEM micrograph of PS spheres, with in the inset the measured size distribution.

Drying effect on PG surface

After slipcasting and drying the concentrated dispersions, a crystalline layer formed on the surface of the sample (see Figure SI.2, b)) due to strong capillary forces between the colloidal spheres. This top layer is undesired for quantitative comparison to the scattering model and was removed after drying by pressing lightly a sheet of paper on top and removing it after. Interestingly, it was found that this top layer enhances the isotropic structural color peaks in the reflectance spectra, as clearly seen in Figure SI.2, c).

Effect of scatterer size on structural color resonances

A series of thirteen samples with varying particle sizes from $r = 57$ nm to $r = 251$ nm was prepared. Figure SI.3 shows a full overview of all experimental and model reflectance spectra as well as photographs and the conversion of the spectra into observable colors.
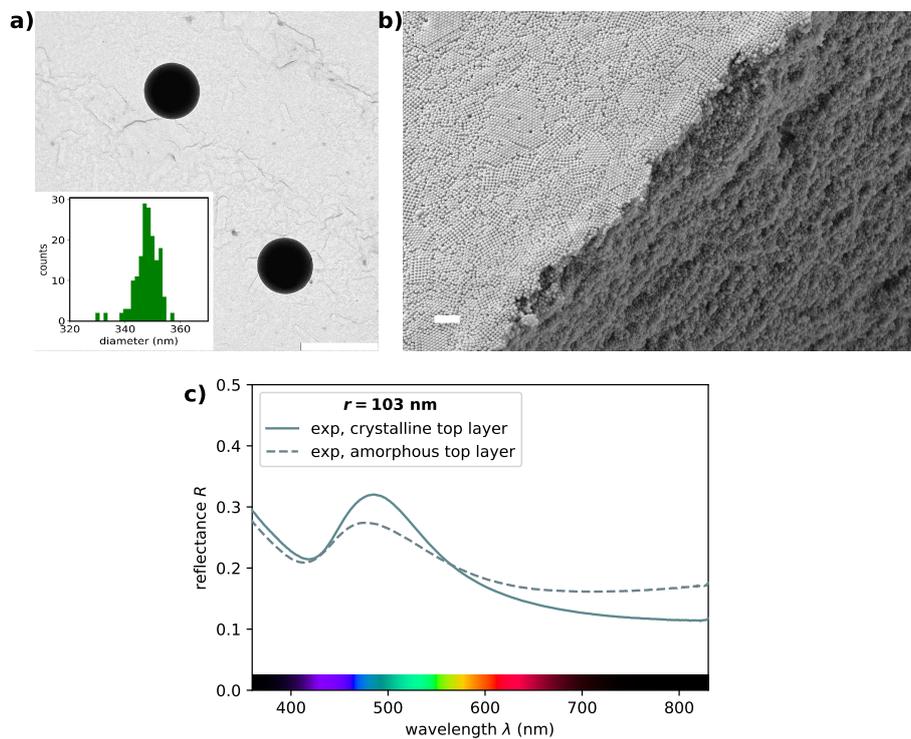
Figure SI.2: a) Typical TEM micrograph of PS spheres with $r = 174 \pm 3$ nm. (Scale bar 500 nm), Inset: Size distribution of the particles as determined with ImageJ. b) SEM micrograph of a sample with particles of radius $r = 250$ nm (scale bar $2\ \mu$m). c) Reflectance spectra of a PGs with particle size $r = 103$ nm with (solid line) and without (dashed line) crystalline monolayer on top.
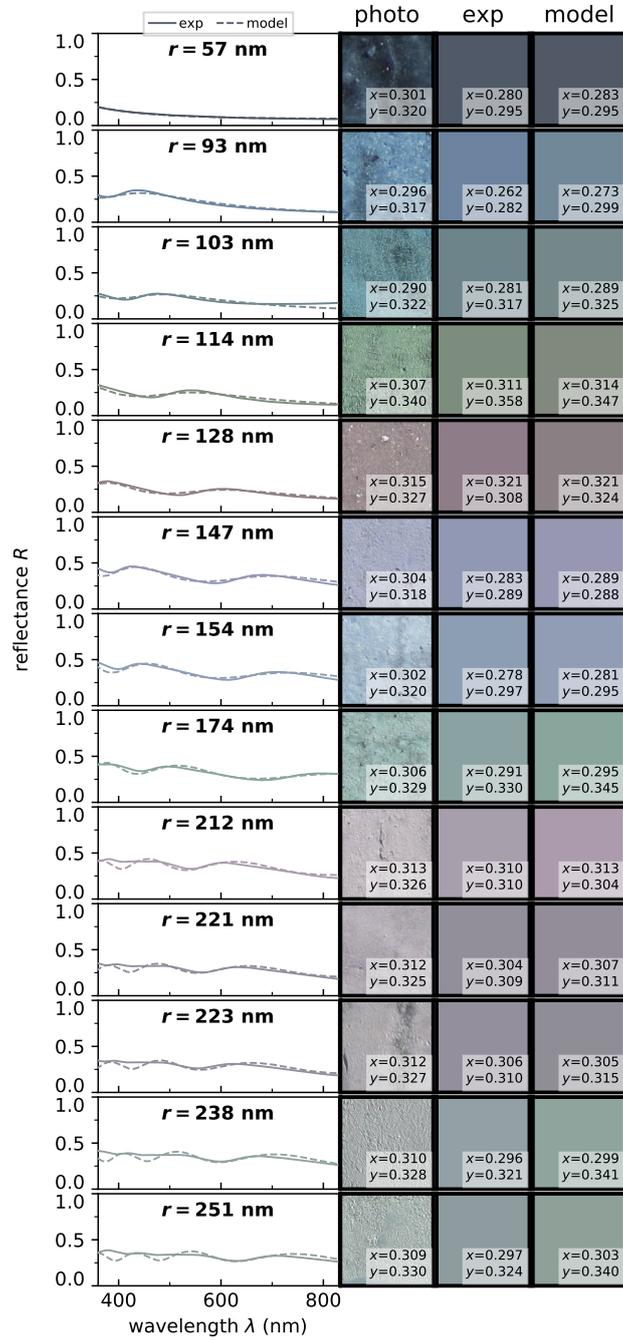
Figure SI.3: Same measurement as in Figure 2(a) for thirteen particle radii.

Spectrum to color conversion

Reflectance $R(\lambda)$ is the ratio of reflected to incident light intensity. Because the perceived color depends on the illumination, the reflectance-to-color conversion accounts for this by multiplying $R(\lambda)$ with a standard white illumination spectrum (Commission internationale de l'éclairage (CIE) Standard Illuminant D_{65}). This spectrum is then converted via the three CIE 1931 2° Standard Observers color matching functions to get the tristimulus in CIE XYZ colorspace. The tristimulus is converted to the normalized CIE xyY colorspace where $x = X/(X + Y + Z)$ and $y = Y/(X + Y + Z)$ are the chromaticity coordinates defining the colors hue and Y is the colors luminance. By normalizing to a certain luminance $Y = 1$, the whole range of colors —called *visible gamut*— can be located in a 2D plane spanned by x and y, see Figure SI.4. Its boundary is determined by the values for single wavelength colors in the visible range, where the endpoints at $\lambda = 360$ nm and $\lambda = 830$ nm are connected by the "line of purples". Any point in this convex area, including the D_{65} whitepoint, can be reached by a linear combination of at least two single line spectra. Color saturation is defined as the distance to this white point.

To print or represent the measured or modeled spectrum as a color on a display, a given xyY-point is further transformed to a linear RGB colorspace. This needs the definition of three primaries (red, green and blue) spanning the space: we use the ITU-R BT.709 standard phosphor chromaticities.[4] Note that these might differ from one displaying device to another, giving rise to potential color distortion. The RGB space is a subspace of the CIE xyY color space because the R, G and B points can only span a space inside of the visible gamut. Colors outside of this space will not be displayed correctly as the saturation stays constant with further distance to the whitepoint. The visible gamut and a color approximation of each xy-point is displayed in Figure SI.4, along with the single line spectra colors, the R, G and B primaries as well as a projection of the RGB space they are spanning.
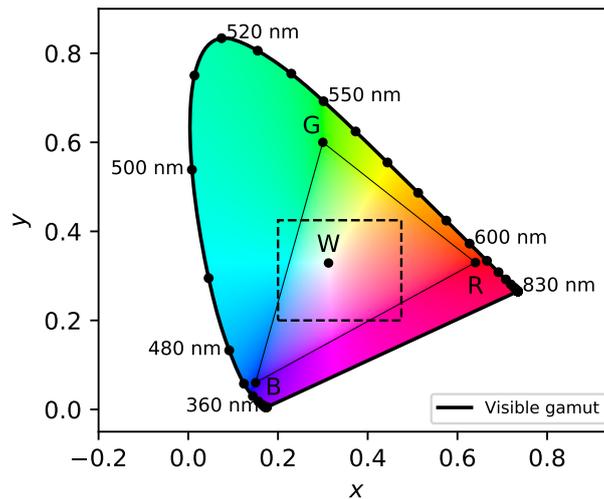
Figure SI.4: CIE xy chromaticity diagram with the RGB primaries and the subspace they are spanning. W denotes the D_{65} whitepoint. The visible gamut boundary arises from the single wavelength colors (annotated black line). The dashed rectangle shows the region of interest zoomed in in Figure 3, c) and d).

[1] G. J. Aubry, L. Schertel, M. Chen, H. Weyer, C. M. Aegerter, S. Polarz, H. Cölfen, G. Maret. *Phys. Rev. A* **2017**, *96*, 4 043871.

[2] L. Schertel, I. Wimmer, P. Besirske, C. M. Aegerter, G. Maret, S. Polarz, G. J. Aubry. *Phys. Rev. Materials* **2019**, *3* 015203.

[3] K. Busch, C. M. Soukoulis. *Phys. Rev. B* **1996**, *54* 893.

[4] Parameter values for the HDTV standards for production and international programme exchange . Standard, International Telecommunication Union, Geneva, CH, **2015**.